

Hadronic Invariant Mass Spectrum in $B \rightarrow X_u l \nu$ Decay with Lepton Energy Cut

K. K. Jeong ^a, C. S. Kim ^{a,b*} and Yeong Gyun Kim ^c

a : Department of Physics, Yonsei University and IPAP, Seoul 120-749, Korea

b : Department of Physics, University of Wisconsin, Madison, WI 53706, USA

c : YITP, Kyoto University, Kyoto 606-8502, Japan

(November 23, 2018)

Abstract

We discuss the implications of charged lepton energy cut to the hadronic invariant mass spectrum in charmless semileptonic B decays. Charged-lepton energy cut is inevitable in order to remove secondary leptonic events such as $b \rightarrow c, \tau \rightarrow l$, and to identify the charged leptons at detectors experimentally. We consider three possible lepton energy cuts, $E_l^{\text{cuts}} = 0.6, 1.5, 2.3$ GeV, and found that with the most probable cuts $E_l^{\text{cut}} = 1.5$ GeV and $M_X^{\text{max}} = 1.5$ (1.86) GeV, 45 \sim 60% (58 \sim 67%) of decay events survive. Therefore, $B \rightarrow X_u l \nu$ decay events can be efficiently distinguished from $B \rightarrow X_c l \nu$ decay events. We also discuss the possible model dependence on the results.

Typeset using REVTeX

*kim@kimcs.yonsei.ac.kr, <http://phya.yonsei.ac.kr/~cskim/>

I. INTRODUCTION

The determination of the CKM parameter $|V_{ub}|$ is important for constructing the so-called unitary triangle. It is hard to determine $|V_{ub}|$ from semileptonic B -meson decays because Cabibbo dominated decay mode $B \rightarrow X_c l \nu$ obscures the $B \rightarrow X_u l \nu$ mode. The traditional method for extracting $|V_{ub}|$ from experimental data involves a study of the charged lepton energy spectrum in inclusive semileptonic B decays, $B \rightarrow X_{u,c} l \nu$ [1]. The $b \rightarrow u$ events are selected above charm threshold, *i.e.* for lepton energies E_l above $(M_B^2 - M_D^2)/(2M_B) \approx 2.3$ GeV. However, this cut on E_l is not very efficient (only less than 10% of $b \rightarrow u$ events survive) and also the dependence of the lepton energy spectrum on perturbative and non-perturbative QCD corrections is the strongest in this end-point region [2–6].

As an alternative, the determination of $|V_{ub}|$ may come from the measurement of the hadronic invariant mass spectrum [7] in the region $M_X < M_D$. For $B \rightarrow X_c l \nu$ decays, one necessarily has $M_X > M_D = 1.86$ GeV. Therefore, if we impose a condition $M_X < M_D$, the resulting events come only from $B \rightarrow X_u l \nu$ decay and most of the $B \rightarrow X_u l \nu$ decays are expected to lie in this region. There is an experimental problem to be expected, though – the charm-leaking of misidentified charmed particles below the kinematic $b \rightarrow c$ threshold. To avoid this leakage, one may concentrate on hadronic invariant mass below a certain value $M_X^{\max} (< M_D)$, say $M_X^{\max} = 1.5$ GeV. The detailed studies of this method were performed in Refs. [8–10]. The integrated fraction of events was introduced,

$$\Phi(M_X^{\max}) = \frac{1}{\Gamma(B \rightarrow X_u l \nu)} \int_0^{M_X^{\max}} dM_X \frac{d\Gamma}{dM_X}, \quad (1)$$

and studied in its sensitivity to the three basic parameters, μ_π^2 , m_b and α_s .

However, we cannot apply the above results to the experimental data directly. From the practical point of view, the leptons with low energy, *i.e.* less than 0.6 GeV, cannot be experimentally identified within the detectors. And also a larger lepton energy cut might be needed to select ‘prompt leptonic events’ ($b \rightarrow l$) from ‘secondary leptonic events’ ($b \rightarrow c \rightarrow l$, $\tau \rightarrow l$). An experimental method such as the technique of neutrino reconstruction [11], which would be used to measure hadronic invariant mass directly and inclusively, may require a lower cut on the charged lepton energy. Therefore, the hadronic invariant mass spectrum would be affected by the various lepton energy cuts. In this Letter, we study the effects of lepton energy cut on

the hadronic invariant mass spectrum in inclusive charmless semileptonic B decays and discuss their implications.

II. DIFFERENTIAL DECAY RATE

At the parton level, the most general hadronic tensor for $B \rightarrow X_u l \nu$ is given by

$$\begin{aligned} W_{\mu\nu}(p, v) = & W_1(v \cdot p, p^2)(p_\mu v_\nu + p_\nu v_\mu - g_{\mu\nu} v \cdot p - i\epsilon_{\mu\nu\alpha\beta} p^\alpha v^\beta) \\ & - W_2(v \cdot p, p^2)g_{\mu\nu} + W_3(v \cdot p, p^2)v_\mu v_\nu \\ & + W_4(v \cdot p, p^2)(p_\mu v_\nu + p_\nu v_\mu) + W_5(v \cdot p, p^2)p_\mu p_\nu . \end{aligned} \quad (2)$$

Here v is the b -quark velocity and p is the total parton momentum. The total momentum carried by the leptons is $q = m_b v - p$. At the tree level, $W_1 = 2\delta(p^2)$ and all other $W_{i \neq 1} = 0$. We follow the $O(\alpha_s)$ corrections to the hadronic tensor from the paper of De Fazio and Neubert [10]. Introducing the scaling variables

$$x \equiv \frac{2E_l}{m_b} , \quad \hat{p}^2 \equiv \frac{p^2}{m_b^2} \quad \text{and} \quad z \equiv \frac{2v \cdot p}{m_b} , \quad (3)$$

where E_l is the charged-lepton energy which is defined in the B -meson rest frame, the triple differential decay rate is given by

$$\begin{aligned} \frac{d^3\Gamma}{dx dz d\hat{p}^2} = & 12\Gamma_0 \left\{ (1 + \bar{x} - z)(z - \bar{x} - \hat{p}^2) \frac{m_b^2}{2} W_1 + (1 - z + \hat{p}^2) \frac{m_b}{2} W_2 \right. \\ & \left. + (\bar{x}(z - \bar{x}) - \hat{p}^2) \frac{m_b}{4} (W_3 + 2m_b W_4 + m_b^2 W_5) \right\}, \end{aligned} \quad (4)$$

where $\bar{x} \equiv 1 - x$, and

$$\Gamma_0 = \frac{G_F^2 |V_{ub}|^2 m_b^5}{192\pi^3}. \quad (5)$$

In terms of the parton variables, the total invariant mass of the hadronic final state is given by

$$s_H = p^2 + 2\bar{\Lambda} v \cdot p + \bar{\Lambda}^2, \quad (6)$$

where $\bar{\Lambda} \equiv M_B - m_b$. Using relation (6), and the scaling variables,

$$\hat{s}_H \equiv s_H/m_b^2 \quad \text{and} \quad \epsilon \equiv \bar{\Lambda}/m_b ;$$

we find the following double differential decay rate

$$\frac{d^2\Gamma}{dx d\hat{s}_H} = \int dz \frac{d^3\Gamma}{dx dz d\hat{p}^2} \Big|_{\hat{p}^2 = \hat{s}_H - \epsilon z - \epsilon^2} , \quad (7)$$

where the phase space for the relevant variables is given by

$$\begin{aligned} \frac{\hat{s}_H - \epsilon^2 + \bar{x}^2}{\epsilon + \bar{x}} &\leq z \leq \frac{\hat{s}_H - \epsilon^2}{\epsilon}, \\ \frac{\epsilon(1 + \epsilon) - \hat{s}_H}{\epsilon} &\leq x \leq 1, \\ \text{for } \quad \quad \quad \epsilon^2 &\leq \hat{s}_H \leq \epsilon(1 + \epsilon) ; \end{aligned} \quad (8)$$

$$\begin{aligned} \frac{\hat{s}_H - \epsilon^2 + \bar{x}^2}{\epsilon + \bar{x}} &\leq z \leq 1 - \epsilon + \frac{\hat{s}_H}{1 + \epsilon}, \\ 0 &\leq x \leq \frac{(1 + \epsilon)^2 - \hat{s}_H}{1 + \epsilon}, \\ \text{for } \quad \quad \quad \epsilon(1 + \epsilon) &\leq \hat{s}_H \leq (1 + \epsilon)^2. \end{aligned} \quad (9)$$

If we integrate the above double differential decay rate over the variable x , we get the single differential decay rate for \hat{s}_H

$$\frac{d\Gamma}{d\hat{s}_H} = \int dx \frac{d^2\Gamma}{dx d\hat{s}_H} , \quad (10)$$

which reproduces numerically the result of Ref. [10].

In order to obtain the physical decay distributions, we should also consider the non-perturbative corrections. The physical decay distributions are obtained from convolution of the above parton level spectra with non-perturbative shape function $F(k_+)$, which governs the light-cone momentum distribution of the heavy quark inside the B -meson [5,6]. The convolution of parton spectra with this function is such that for the decay distributions the b -quark mass m_b is replaced by the momentum dependent mass, $m_b + k_+$, and similarly the parameter $\bar{\Lambda} = M_B - m_b$ is replaced by $\bar{\Lambda} - k_+$. Here k_+ can take values between $-m_b$ and $\bar{\Lambda}$, with a distribution centered around $k_+ = 0$ and with a characteristic width of $\mathcal{O}(\Lambda)$. Then, the scaling variables x , \hat{s}_H and ϵ are replaced by the new variables

$$x_q \equiv \frac{2E_l}{M_B - q_+} , \quad \hat{s}_{H,q} \equiv \frac{s_H}{(M_B - q_+)^2} \quad \text{and} \quad \epsilon_q \equiv \frac{q_+}{M_B - q_+} , \quad (11)$$

where $q_+ \equiv \bar{\Lambda} - k_+$. The physical double differential decay rate for the charged-lepton energy and the hadronic invariant mass is given by

$$\frac{d^2\Gamma}{dE_l ds_H} = 2 \int_0^{q_+^{\max}} dq_+ \frac{F(\bar{\Lambda} - q_+)}{(M_B - q_+)^3} \frac{d\Gamma}{dx d\hat{s}_H}(x_q, \hat{s}_{H,q}, \epsilon_q), \quad (12)$$

where $q_+^{\max} = \min(M_B - 2E_l, \sqrt{s_H})$. Finally, the physical distribution for the hadronic invariant mass can be obtained in two different ways;

$$\frac{d\Gamma}{ds_H} = \int dE_l \frac{d^2\Gamma}{dE_l ds_H} \quad (13)$$

$$= \int_0^{\sqrt{s_H}} dq_+ \frac{F(\bar{\Lambda} - q_+)}{(M_B - q_+)^2} \frac{d\Gamma}{d\hat{s}_H}(\hat{s}_{H,q}, \epsilon_q), \quad (14)$$

which should give the same results. We note that, after the implementation of such Fermi motion, now the kinematic variables take values in the entire phase space determined by hadron kinematics, *i.e.* $0 \leq E_l \leq M_B/2$ and $0 \leq s_H (\equiv M_X^2) \leq M_B^2$. Eqs. (12-14) are our starting point for the numerical calculations.

III. NUMERICAL ANALYSES AND CONCLUSIONS

To perform the numerical calculation we should choose a specific form for the shape function $F(k_+ \equiv \bar{\Lambda} - q_+)$. It is subject to the constraints on the moments of the function

$$A_n = \langle k_+^n \rangle \equiv \int dk_+ k_+^n F(k_+),$$

which are given by the expectation values of local heavy quark operators. In practice we know only the size of the first few moments; one finds

$$A_0 = 1, \quad A_1 = 0 \quad \text{and} \quad A_2 = \frac{1}{3} \mu_\pi^2, \quad (15)$$

where μ_π^2 is the average momentum squared of the b quark inside the B -meson. The parameters $\bar{\Lambda}$ and μ_π^2 were obtained by the HQET and QCD sum rules in Refs. [12,13];

$$\bar{\Lambda} = 0.4 \sim 0.6,$$

$$\mu_\pi^2 = 0.6 \pm 0.1 \quad [12] \quad \text{or} \quad \mu_\pi^2 = 0.10 \pm 0.05 \quad [13]. \quad (16)$$

One then chooses some reasonable ansatz for $F(k_+)$; its parameters are adjusted so as to reproduce its known moments. Several functional forms for this function have been suggested in the literature [6,14–16]. We adopt the simple form of Ref. [16],

$$F(k_+) = N(1-x)^a e^{(1+a)x} \quad \text{with} \quad x = \frac{k_+}{\Lambda} \leq 1, \quad (17)$$

which is such that $A_1 = 0$ by construction (neglecting exponentially small terms in m_b/Λ), whereas the condition for A_0 fixes the normalization N . The parameter a can be related to the second moment, yielding $A_2 = \bar{\Lambda}^2/(1+a)$. A typical choice of values is $m_b = 4.8 \text{ GeV}$ and $a = 1.29$, corresponding to $\bar{\Lambda} \approx 0.48 \text{ GeV}$ and $\mu_\pi^2 \approx 0.3 \text{ GeV}^2$. Below, we keep the parameter ‘ a ’ fixed, and consider the three choices $m_b = 4.65, 4.8$ and 4.95 GeV . These choices correspond to the following sets,

$$(\bar{\Lambda}(\text{GeV}), \mu_\pi^2(\text{GeV}^2)) = (0.63, 0.52), \quad (0.48, 0.30) \quad \text{and} \quad (0.33, 0.14), \quad (18)$$

respectively. We fix the QCD coupling $\alpha_s = 0.22$.

Now the calculation of the hadronic invariant mass spectrum is straightforward. The 3-dimensional plot of double differential decay rate,

$$\frac{d\Gamma}{dM_X dE_l} = 2M_X \frac{d\Gamma}{ds_H dE_l} \quad (19)$$

is shown in Fig. 1, with $m_b = 4.8 \text{ GeV}$. The lines in the bottom plane show the contour lines. The three straight lines in contour figure, which are the projections of three curved lines in the 3-dimensional figure, indicate the charged-lepton energy cuts, *i.e.* $E_l^{\text{cut}} = 0.6, 1.5, 2.3 \text{ GeV}$, respectively. From the figure, one can find that a significant fraction ($\sim 90\%$) of the decay events lie below the charmed states, *i.e.* have $M_X < 1.86 \text{ GeV}$. This is in sharp contrast with the usual cut on charged-lepton energy E_l . Due to measurement errors, there will be a tail from $b \rightarrow c$ decays below M_D . To avoid this leakage, one can concentrate on hadronic invariant masses below a certain value $M_X^{\text{max}} < M_D$. With a lower cutoff on M_X (say $M_X^{\text{max}} = 1.5 \text{ GeV}$ or 1.6 GeV), the majority of decays still appears below the M_X^{max} region.

But in reality we cannot apply the above results to experimental data directly. In $B \rightarrow X l \nu$ semileptonic decay experiment, the secondary electrons such as $b \rightarrow c \rightarrow l$ cascade decay contaminates the signal of the pure $B \rightarrow X_c l \nu$ decay. The secondary electrons have typically lower energy than the primary electrons because the mass of D -meson is much less than the mass of B -meson. Therefore, only the electrons with energy greater than 1.5 GeV can be considered to be purely from $B \rightarrow X_{c,u} l \nu$. Using the double lepton tagging method, one can reconstruct the primary leptons with energy less than 1.5 GeV [17]. But in this method, both

B -mesons from $\Upsilon(4S)$ should decay semileptonically. So it gives much less data samples. Also the experimental method such as neutrino reconstruction technique, which would be used to measure the hadronic invariant mass inclusively, requires a lower cut on the charged lepton energy. Therefore, we apply the charged-lepton energy cuts $E_l^{\text{cut}} = 0.6, 1.5, 2.3$ GeV on the hadronic invariant mass spectrum. The cut $E_l^{\text{cut}} = 0.6$ GeV corresponds to the double lepton tagging data, and $E_l^{\text{cut}} = 1.5$ GeV corresponds to the normal single lepton tagging data. We also apply $E_l^{\text{cut}} = 2.3$ GeV to compare the data with the previously measured charged lepton energy data as the kinematic boundary to separate the signal from $b \rightarrow cl\nu$ decay.

Fig. 2 shows the hadronic invariant mass distribution with varying m_b mass as 4.65, 4.8, 4.95 GeV. It is normalized in units of $(|V_{ub}|^2 \times \text{GeV})$. Note that in the $b \rightarrow u$ semileptonic decay, the leptons have quite large energies so that M_X distribution with $E_l^{\text{cut}} = 0.6$ GeV is not much different from the distribution without any lepton energy cut. In the case of $E_l^{\text{cut}} = 2.3$ GeV, we can see that there is no decay event above $M_X \geq 1.86$ GeV. This is consistent with the kinematics that leptons with energy greater than 2.3 GeV are purely from $b \rightarrow ul\nu$ decay. And also we can see that this lepton energy cut is very inefficient because only a small part of the decays survive this cut, as mentioned earlier.

Fig. 3 shows the integrated decay rate up to M_X^{max} ,

$$\Gamma(M_X^{\text{max}}) = \int_0^{M_X^{\text{max}}} dM_X \frac{d\Gamma}{dM_X}. \quad (20)$$

The numerical values are summarized in Tables I, II and III. Here we can see that if we consider total decay rate with $E_l^{\text{cut}} = 2.3$ GeV, only $9 \sim 14\%$ of decay events remain. When we use $M_X^{\text{max}} = M_D$ cut, $82 \sim 94\%$ of decay events remain without any lepton energy cut, and $79 \sim 92\%$ ($58 \sim 67\%$) of decay events survive for $E_l^{\text{cut}} = 0.6$ (1.5) GeV. In this case, there might be a difficulty to draw the reliable conclusion because of the possible charm-leaking. However, even in this case, the hard lepton energy cut may be helpful to reduce the contamination from the charm-leaking because the lepton energy of $B \rightarrow X_c l \nu$ decays is softer compared to that of $B \rightarrow X_u l \nu$ decays. If we further reduce the maximum value of M_X , *i.e.* $M_X^{\text{max}} = 1.5$ GeV, $60 \sim 81\%$ of the events remain without lepton energy cut, and $59 \sim 80\%$ ($45\% \sim 60\%$) of the events survive for $E_l^{\text{cut}} = 0.6$ (1.5) GeV. As we mentioned previously, in the case of $E_l^{\text{cut}} = 0.6$ GeV, both B -mesons should decay semileptonically to be identified as prompt leptonic events. Since $E_l^{\text{cut}} = 2.3$ GeV gives only $\sim 10\%$ of the total decay rate, the cut

$E_l^{\text{cut}} = 1.5$ GeV would be our best option.

Now we discuss the dependence of the results on the various input parameters and the choice of the universal distribution function. The dependence on μ_π^2 is found not so significant, compared to the $\bar{\Lambda}$ (or equivalently m_b) dependence. The decay rates with the parameters $m_b = 4.8$ GeV and $\mu_\pi^2 = 0.6$ GeV² are shown in Table IV. By comparing Table IV with Tables I, II and III, we can see that the main uncertainty in decay rates comes from the uncertainty in $\bar{\Lambda}$ (or m_b). The dependence of the result on the α_s variation could be quite large since the perturbative correction to the total decay rate is linear with the parameter α_s , and the size of α_s correction is almost 20% of the leading approximation. From Tables I, II, III and V, we can see that the effects of the variation of α_s from 0.22 to 0.35, with fixed $m_b = 4.8$ GeV, are similar to the case of the variation of m_b from 4.8 to 4.65 GeV, with fixed $\alpha_s = 0.22$.

Next, in order to estimate the possible dependence of the results on the choice of universal distribution function, we adopt ACCMM [18] model-induced distribution function [6,15],

$$F_{\text{ACCMM}}(q_+) = \frac{1}{\sqrt{\pi}} \frac{1}{p_F} \exp \left\{ -\frac{1}{4} \left[\frac{m_{sp}^2}{p_F q_+} - \frac{q_+}{p_F} \right]^2 \right\}. \quad (21)$$

As seen, this shape function is dependent on the two parameters, p_F and m_{sp} . We choose the three sets,

$$(p_F, m_{sp}) = (0.504, 0.251), \quad (0.383, 0.193) \quad \text{and} \quad (0.262, 0.136) \quad (\text{in units of GeV}),$$

which respectively correspond to the above three choices of $m_b = 4.65, 4.8$ and 4.95 GeV with fixed ‘ a ’ of Eq. (17). The integrated decay rates $\Gamma(M_X^{\text{max}})$ are summarized in Tables VI and VII. The resulting decay rates are almost the same as the corresponding results of Tables I and III. The differences in the decay rate for two universal distribution functions are within 2% only.

Finally we note that the results would be affected by some resonance effects around M_X^{max} . The real result would be a sum of all the exclusive decays in which a few resonances dominate at some specific M_X ’s, so the actual M_X distribution will be with humps and bumps, while our results are smoothed inclusive results using the duality. However, our integrated results would be quite correct, once there is no significant resonance around the region of M_X cut. If M_X^{max} is around 1 GeV, then there are a few important resonances, but if M_X is large enough, *e.g.* 1.5

GeV, then there is no significant resonance from $b \rightarrow u$, but rather there will be decays with many pions.

In summary, we investigated the effects of charged lepton energy cut on the hadronic invariant mass spectrum for $B \rightarrow X_u l \nu$ decays and their implications. As is well known, the charged-lepton energy cut is experimentally inevitable in order to remove secondary leptonic events such as $b \rightarrow c \rightarrow l, \tau \rightarrow l$, and to identify the charged leptons at detectors. We found that with $E_l^{\text{cut}} = 1.5$ GeV and $M_X^{\text{max}} = 1.5$ (1.86) GeV, 45 \sim 60% (58 \sim 67%) of decay events survive, and with $E_l^{\text{cut}} = 0.6$ GeV and $M_X^{\text{max}} = 1.5$ (1.86) GeV, 59 \sim 80% (79 \sim 92%) survive. Finally without E_l^{cut} , 60 \sim 81% (82 \sim 94%) of decay events survive with $M_X^{\text{max}} = 1.5$ (1.86) GeV. Therefore, $B \rightarrow X_u l \nu$ decay events can be efficiently distinguished from $B \rightarrow X_c l \nu$ decay events by using the hadronic recoil mass and the charged lepton energy together.

ACKNOWLEDGMENTS

We thank G. Cvetic for careful reading of the manuscript and his valuable comments. The work of C.S.K. was supported in part by the BSRI Program of MOE, Project No. 99-015-DI0032, and in part by the KRF Sughak-research program, Project No. 1997-011-D00015. The work of K.K.J. was supported by Brain Korea 21 Project and by the KOSEF through Grant No. 1999-2-111-002-5. The work of Y.G.K is supported by JSPS.

REFERENCES

- [1] F. Bartelt *et al.*, CLEO Collaboration, Phys. Rev. Lett. **71**, 4111 (1993); H. Albrecht *et al.*, Argus Collaboration, Phys. Lett. **B255**, 297 (1991).
- [2] N. Cabibbo, G. Corbo and L. Maiani, Nucl. Phys. **B155**, 93 (1979); *ibid.* **B212**, 99 (1983); M. Jezabek and J. H. Kuhn, *ibid.* **B320**, 20 (1989); A. Czarnecki and M. Jezabek, *ibid.* **B427**, 3 (1994).
- [3] J. Chay, H. Georgi and B. Grinstein, Phys. Lett. **B247**, 399 (1990); I.I. Bigi, M.A. Shifman, N.G. Uraltsev and A.I. Vainshtein, Phys. Rev. Lett. **71**, 496 (1993); T. Mannel, Nucl. Phys. **B413**, 396 (1994).
- [4] A. V. Manohar and M. B. Wise, Phys. Rev. **D49**, 1310 (1994); B. Blok, L. Koyrakh, M. Shifman and A. I. Vainstein, Phys. Rev. **D49**, 3356 (1994).
- [5] M. Neubert, Phys. Rev. **D49**, 3392 (1994); *ibid* 4623 (1994).
- [6] I. I. Bigi, M. A. Shifman, N. G. Uraltsev and A. L. Vainstein, Int. J. Mod. Phys. **A9**, 2467 (1994); Phys. Lett. **B328**, 431 (1994).
- [7] V. Barger, C. S. Kim and G. Phillips, Phys. Lett. **B251**, 629 (1990)
- [8] R. D. Dikeman and N. G. Uraltsev, Nucl. Phys. **B509**, 378 (1998); I. Bigi, R. D. Dikeman and N. G. Uraltsev, Eurr. Phys. J. **C4**, 453 (1998).
- [9] A. Falk, Z. Ligeti and M. Wise, Phys. Lett. **B406**, 225 (1997).
- [10] F. De Fazio and M. Neubert, JHEP9906, 017 (1999).
- [11] J. Alexander *et al.*, CLEO Collaboration, Phys. Rev. Lett. **77**, 5000 (1996).
- [12] P. Ball and V. M. Braun, Phys. Rev. **D49**, 2472 (1994); I. I. Bigi, M. A. Shifman, N. G. Uraltsev and A.I. Vainshtein, Phys. Rev. **D52**, 196 (1995); E. Bagan, P. Ball, V. M. Braun and P. Gosdzinsky, Phys. Lett. **B342**, 362 (1995); D. S. Hwang, C. S. Kim and W. Namgung, Phys. Rev. **D54**, 5620 (1996); Phys. Lett. **B406**, 117 (1997); F. de Fazio, Mod. Phys. Lett. **A11**, 2693 (1996); H. Li and H. Yu, Phys. Rev **D55**, 2833 (1997); K. K. Jeong and C. S. Kim, Phys. Rev. **D59**, 114019 (1999).

- [13] A. Kapustin, Z. Ligeti and M. B. Wise, B. Grinstein, Phys. Lett. **B375**, 327 (1996); M. Gremm , A. Kapustin, Z. Ligeti and M. B. Wise, Phys. Rev. Lett. **77**, 20 (1996); M. Neubert, Phys. Lett. **B389**, 727 (1996).
- [14] K. Y. Lee and J. K. Kim, Phys. Lett. **B377**, 153 (1996).
- [15] C. S. Kim, Y. G. Kim and K. Y. Lee, Phys. Rev. **D57**, 4002 (1998).
- [16] A. L. Kagan and M. Neubert, Eur. Phys. J. **C7**, 5 (1999).
- [17] CLEO Collaboration: B. Barish *et al.*, Phys. Rev. Lett. **76**, (1996) 1570.
- [18] G. Altarelli et al., Nucl. Phys. **B208** (1982) 365.

TABLES

TABLE I. Γ_{total} with charged-lepton energy cuts with fixed $\alpha_s = 0.22$ and $a = 1.29$. The values of $m_b = 4.65, 4.8, 4.95$ GeV correspond to the set of values of Eq. (18) for $\bar{\Lambda}, \mu_\pi^2$.

$m_b(\text{GeV})$	$E_l^{\text{cut}}(\text{GeV})$	$\Gamma_{\text{total}}(V_{ub} ^2 \text{ GeV})$	percentage
4.8	0	0.503	100%
	0.6	0.489	97%
	1.5	0.336	67%
	2.3	0.054	11%
4.65	0	0.442	100%
	0.6	0.429	97%
	1.5	0.287	65%
	2.3	0.039	9%
4.95	0	0.574	100%
	0.6	0.560	98%
	1.5	0.395	69%
	2.3	0.079	14%

TABLE II. $\Gamma(M_X^{\max} = 1.86\text{GeV})$ with charged-lepton energy cuts.

$m_b(\text{GeV})$	$E_l^{\text{cut}}(\text{GeV})$	$\Gamma(M_X^{\max} = 1.86 \text{ GeV})(V_{ub} ^2 \text{ GeV})$	percentage
4.8	0	0.442	88%
	0.6	0.432	86%
	1.5	0.312	62%
	2.3	0.054	11%
4.65	0	0.359	82%
	0.6	0.351	79%
	1.5	0.254	58%
	2.3	0.039	9%
4.95	0	0.538	94%
	0.6	0.526	92%
	1.5	0.381	67%
	2.3	0.079	14%

TABLE III. $\Gamma(M_X^{\max} = 1.50\text{GeV})$ with charged-lepton energy cuts.

$m_b(\text{GeV})$	$E_l^{\text{cut}}(\text{GeV})$	$\Gamma(M_X^{\max} = 1.50 \text{ GeV})(V_{ub} ^2 \text{ GeV})$	percentage
4.8	0	0.348	69%
	0.6	0.342	67%
	1.5	0.261	52%
4.65	0	0.263	60%
	0.6	0.259	59%
	1.5	0.200	45%
4.95	0	0.465	81%
	0.6	0.457	80%
	1.5	0.343	60%

TABLE IV. $\Gamma(M_X^{\max})$ with charged-lepton energy cuts ($m_b = 4.8$ GeV and $\mu_\pi^2 = 0.6$ GeV²).

$M_X^{\max}(\text{GeV})$	$E_l^{\text{cut}}(\text{GeV})$	$\Gamma(M_X^{\max})(V_{ub} ^2 \text{ GeV})$	percentage
no cut	0	0.519	100%
	0.6	0.505	97%
	1.5	0.351	68%
1.86	0	0.460	89%
	0.6	0.450	87%
	1.5	0.329	63%
1.5	0	0.391	75%
	0.6	0.384	74%
	1.5	0.290	56%

TABLE V. $\Gamma(M_X^{\max})$ with charged-lepton energy cuts ($m_b = 4.8$ GeV and $\alpha_s = 0.35$).

$M_X^{\max}(\text{GeV})$	$E_l^{\text{cut}}(\text{GeV})$	$\Gamma(M_X^{\max})(V_{ub} ^2 \text{ GeV})$	percentage
no cut	0	0.441	100%
	0.6	0.429	97%
	1.5	0.292	66%
1.86	0	0.367	83%
	0.6	0.360	82%
	1.5	0.264	60%
1.5	0	0.272	62%
	0.6	0.269	61%
	1.5	0.211	48%

TABLE VI. Γ_{total} with charged-lepton energy cuts (ACMM distribution function of Eq. (21)).

$m_b(\text{GeV})$	$E_l^{\text{cut}}(\text{GeV})$	$\Gamma_{\text{total}}(V_{ub} ^2 \text{ GeV})$	percentage
4.8	0	0.503	100%
	0.6	0.489	97%
	1.5	0.336	67%
	2.3	0.055	11%
4.65	0	0.443	100%
	0.6	0.429	97%
	1.5	0.287	65%
	2.3	0.040	9%
4.95	0	0.573	100%
	0.6	0.558	97%
	1.5	0.394	69%
	2.3	0.079	14%

TABLE VII. $\Gamma(M_X^{\text{max}} = 1.50\text{GeV})$ with charged-lepton energy cuts (ACMM).

$m_b(\text{GeV})$	$E_l^{\text{cut}}(\text{GeV})$	$\Gamma(m_X^{\text{max}} = 1.50 \text{ GeV})(V_{ub} ^2 \text{ GeV})$	percentage
4.8	0	0.351	70%
	0.6	0.345	69%
	1.5	0.263	52%
4.65	0	0.271	61%
	0.6	0.267	60%
	1.5	0.205	46%
4.95	0	0.465	81%
	0.6	0.456	80%
	1.5	0.343	60%

FIGURES

FIG. 1. The 3-dimensional plot of the double differential decay rate $d\Gamma/dE_l dM_X$ with $m_b = 4.8$ GeV. The lines in the bottom plane show the contour lines. The three straight lines in contour figure, which are the projections of three curved lines in the 3-dimensional figure, indicate the charged-lepton energy cuts, *i.e.* $E_l^{\text{cut}} = 0.6, 1.5, 2.3$ GeV, respectively.

FIG. 2. Hadronic invariant mass distribution with $m_b = 4.8, 4.65, 4.95$ GeV and $E_l^{\text{cut}} = 0, 0.6, 1.5, 2.3$ GeV. The four curves with the same line style are corresponding to $E_l^{\text{cut}} = 0, 0.6, 1.5$ and 2.3 GeV, respectively, from top to bottom.

FIG. 3. $\Gamma(M_X^{\text{max}})$ with $m_b = 4.8, 4.65, 4.95$ GeV and $E_l^{\text{cut}} = 0, 0.6, 1.5, 2.3$ GeV, integrated up to M_X^{max} . The four curves with the same line style are corresponding to $E_l^{\text{cut}} = 0, 0.6, 1.5$ and 2.3 GeV, respectively, from top to bottom.

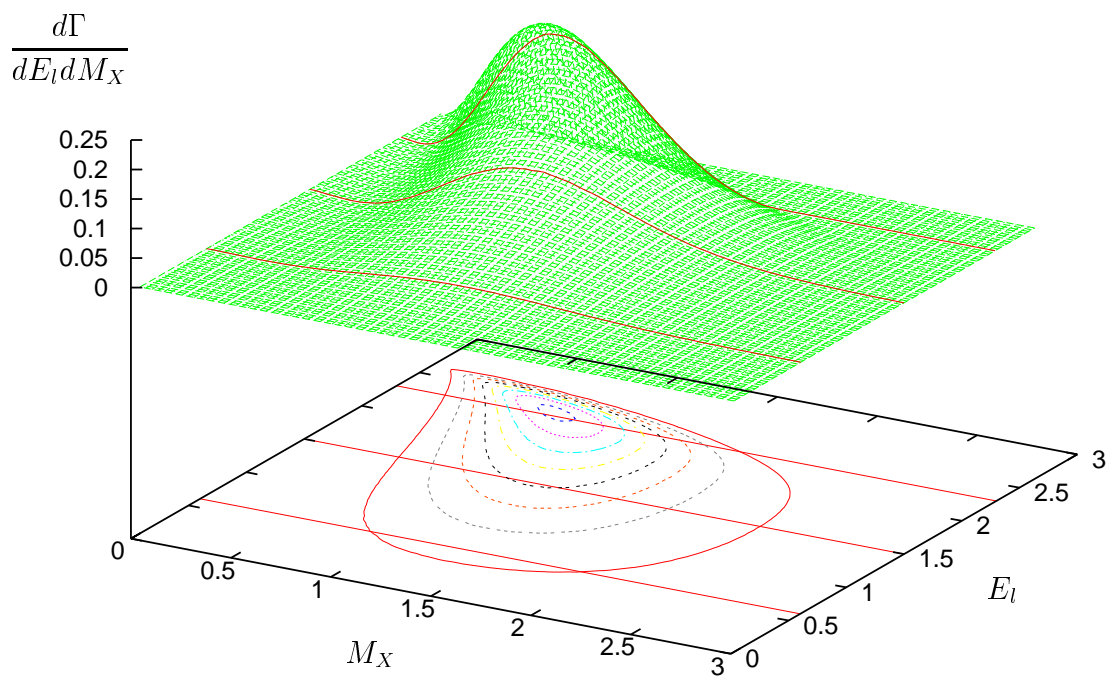


FIG. 1

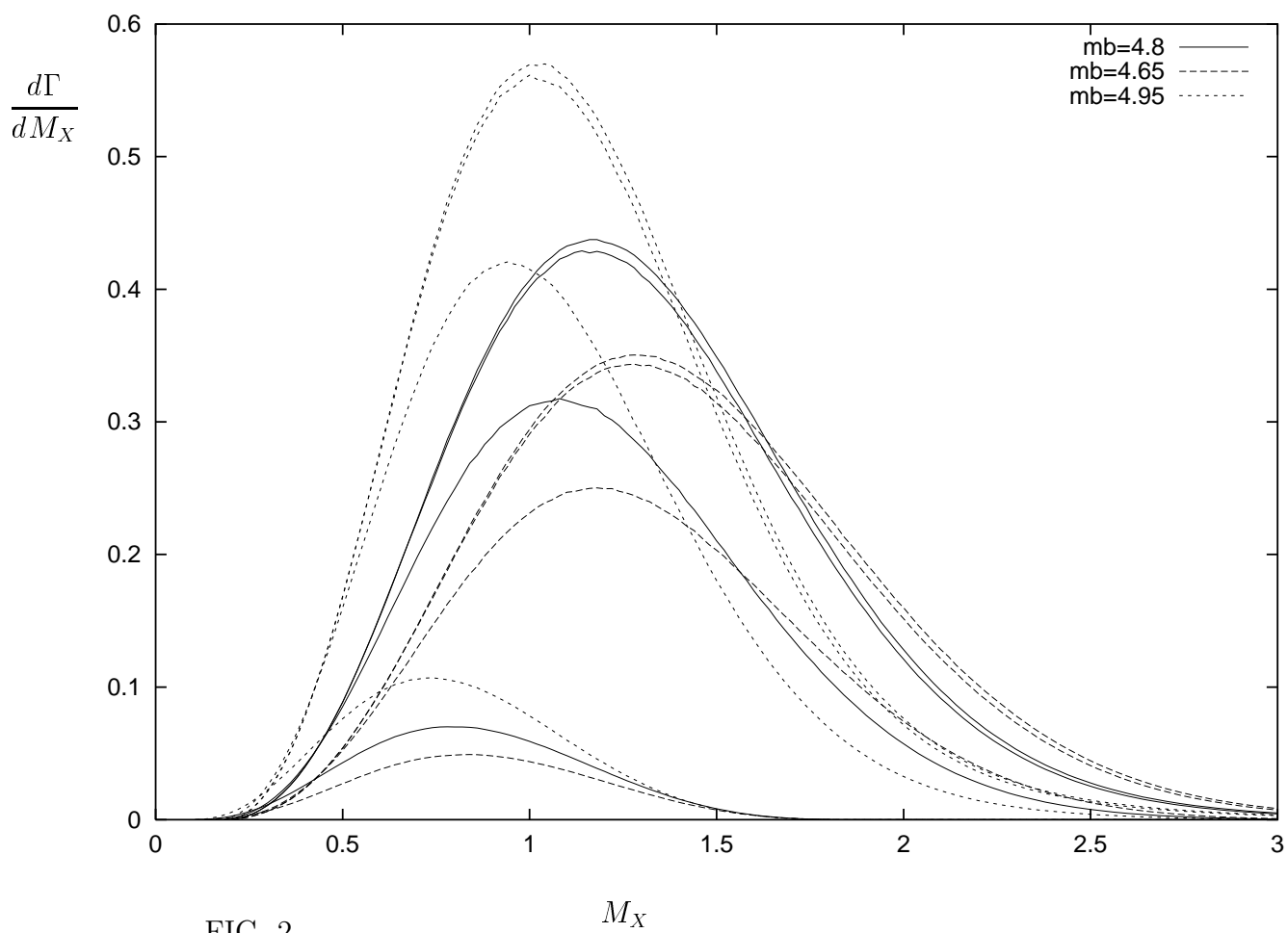


FIG. 2

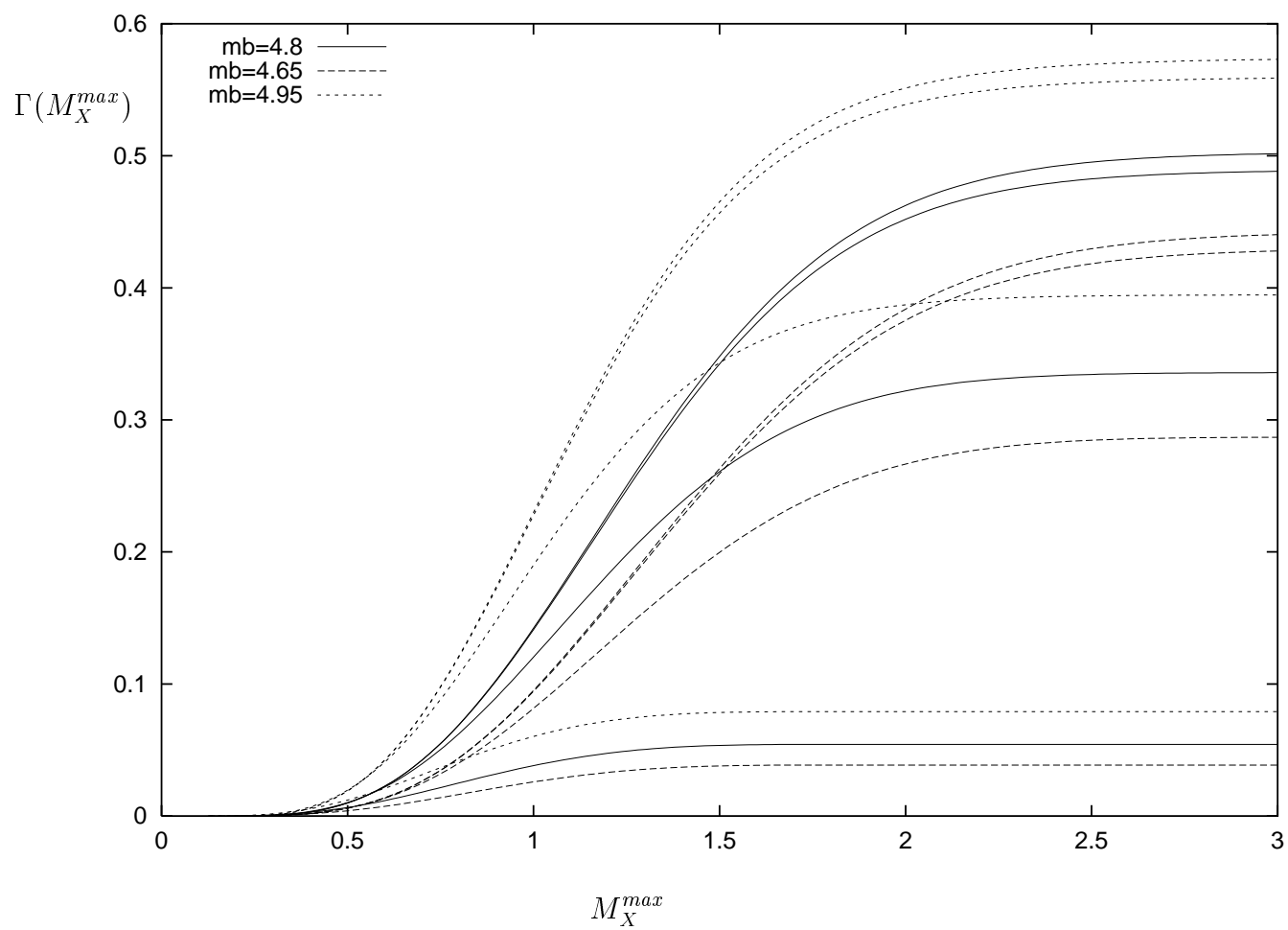


FIG. 3